NATURAL REMANENT MAGNETIZATION OF THE FUSION CRUST OF METEORITES

Takesi NAGATA

National Institute of Polar Research, 9–10, Kaga 1-chome, Itabashi-ku, Tokyo 173

Abstract: Natural remanent magnetization (NRM) of 5 Yamato achondrites and 2 Yamato ordinary chondrites is examined as a function of depth from their surface through the fusion crust into the apparently undisturbed interior. In 5 achondrites, the dark colored fusion crust is much more strongly magnetized in comparison with the uniform NRM of the interior.

The intensity of fusion crust NRM generally decreases inward from the surface down to 0.3–0.8 mm in depth. The intense fusion crust NRM can be interpreted as the thermoremanent magnetization acquired in the geomagnetic field on and after entry into the earth's atmosphere.

The fusion crust NRM of two ordinary chondrites cannot be clearly distinguished from their interior NRM, probably because the latter is competitively strong as the former.

1. Introduction

An anomalously high intensity of natural remanent magnetization (NRM) of the fusion crust of stony meteorites in comparison with NRM of their interior was first found by WEAVING (1962). In a long strip sample of Brewster meteorite (olivine-hypersthene chondrite) stretching from edge to edge of the sample, he found that NRM intensity is about 0.29 emu/gm at the edges while it is constantly about 5×10^{-3} emu/gm in the neighborhood of the center. On the edge surface of this meteorite, a skin (fusion crust) approximately 1 mm thick is present. It seems most likely therefore that the intense NRM of edge parts is due to a certain special magnetization of fusion crust. If the origin of these NRMs is attributed to the thermoremanent magnetization (TRM), the ambient magnetic field is estimated to be about 0.1 and 10.5 Oe for the interior and the fusion crust respectively. Since the AF-demagnetization curve of the interior NRM similar to that of TRM, the interior NRM of Brewster chondrite is attributable to TRM acquired in 0.1 Oe. However, the AF-demagnetization characteristics of the fusion crust NRM are more like those of isothermal remanent magnetization (IRM, acquired in 450 Oe) than those of TRM. Thus, the acquisition mechanism of fusion crust NRM of Brewster chondrite has remained uncertain.

BUTLER (1972) examined NRM of the fusion crust of the Allende carbonaceous chondrite in comparison with its comparatively uniform NRM of its interior part.

In his result, the intensity of NRM in the fusion crust is 1.4×10^{-3} emu/gm, and its direction makes an angle of about 100° with the direction of interior NRM whose intensity is 3.0×10^{-4} emu/gm. The thickness of strongly magnetized crustal layer is about 1 mm or less.

NAGATA and SUGIURA (1977) have recently tried to examine the fusion crust NRM of an achondrite (howardite) in comparison with its interior NRM. In their result, the NRM of a fusion crust of about 0.5 mm in thickness is represented by $I_n=7.6\times10^{-5}$ emu/gm in average intensity and its direction making about 130° in angle with the direction of interior NRM whose average intensity is 6.3×10^{-6} emu/gm. In this case also, the fusion crust NRM is much stronger than the interior NRM. By comparing the TRM acquisition characteristics of the same sample, the strong NRM of the fusion crust has been attributed to TRM acquired in a magnetic field of 0.54 Oe on entry into the earth's atmosphere.

As a large number of meteorites collected from the Yamato Meteorite Ice Field have the fusion crusts, characteristics of the fusion-crust NRM of typical Yamato stony meteorites have been specifically examined with reference to those of their interior NRM in the present work, for the purpose of approaching this unestablished problem in regard to the origin of fusion-crust NRM of meteorites.

2. General Descriptions of Meteorite Samples

Five achondrites covered by the fusion crust are selected for the present experimental examinations. They are Yamato-74037 (diogenite; original weight= 592 gm), Yamato-74159 (eucrite; original weight=98.2 gm), Yamato-74450 (eucrite; original weight=236 gm), Yamato-75032 (diogenite; original weight= 189 gm) and Yamato-7308(*l*) (howardite; original weight=480 gm). The petrographical and mineralogical characteristics of Yamato-74037, -74159, -74450 and -75032 achondrites are described in fair detail by TAKEDA *et al.* (1978), and those of Yamato-7308(*l*) by YAGI *et al.* (1978). The bulk chemical compositions of silicate phases and troilite have been analyzed for Yamato-74159, -74450 and -75032 (TAKEDA *et al.*, 1978) as given in Table 1, but their metal phase composition has not yet been known. The bulk chemical composition of Yamato-7308(*l*) is given also in Table 1 (YAGI *et al.*, 1978).

The bulk chemical composition and mineralogical structures of Yamato-74159 and -74450 are those of an eucrite, and those of Yamato-75032 indicate that it is an iron-rich diogenite (TAKEDA *et al.*, 1978), while Yamato-74037 is a diogenite which has chemical composition and texture almost the same as Yamato-692(b) diogenite. According to YAGI *et al.* (1978), on the other hand, Yamato-7308(*l*) is most magnesian among the howardites ever reported.

The basic magnetic properties of these five achondrites, such as saturation magnetization (I_s), saturation remanent magnetization (I_R), coercive force (H_c)

Table 1. Bulk chemical composition.

	Yamato				
	-74450	-74159	-75032 (wt.%)	-7308 (*l*)	-74646
(Silicate phase)					
SiO_2	49.36	49.04	51.92	51.06	40.26
MgO	8.06	8.29	20.99	22.02	25.11
FeO	18.26	19.23	18.85	16.00	19.02
Al_2O_3	10.82	10.35	2.28	3.64	3.97
CaO	9.52	9.48	3.31	3.50	1.72
Na_2O	0.51	0.58	0.12	0.16	0.97
K_2O	0.06	0.07	0.04	0.06	0.13
Cr_2O_3	0.33	0.44	0.72	0.68	0.78
MnO	0.51	0.53	0.55	0.57	0.37
TiO_2	1.04	1.09	0.40	0.22	0.15
P_2O_5	0.10	0.07	0.03	0.01	0.25
$H_2O(+)$	0.35	0.32	0.32	—	0.04
$H_2O(-)$	0.00	0.00	0.00	—	0.00
NiO	0.003	0.003	0.003	—	—
(Metal phase)					
Fe	—	—	—	0.39	1.96
Ni	—	—	—	0.0115	1.01
Co	<0.003	<0.003	<0.003	0.007	0.031
(Sulfide phase)					
FeS	0.64	0.15	0.30	0.75	4.59
Total	99.56	99.65	99.83	99.62	

(Analyzed by H. HARAMURA)

and remanence coercive force (H_{Rc}) are given in Table 2. As shown in this table, the content of native iron is particularly small in Yamato-74159 and -75032.

The fusion crusts of two ordinary chondrites also have been examined for comparison. The two samples are Yamato-74362 (L_6 chondrite: original weight= 4175 gm) and Yamato-74646 (LL_5 chondrite: original weight=554 gm).

According to FREDERIKSSON (1977, private communication), Yamato-74362 is an L_6 chondrite, in which the olivine composition is represented by 24 mol% of fayalite. A preliminary analysis of olivine and pyroxene of Yamato-74646 carried out by YANAI *et al.* (1978) has shown that the mean composition of olivine is represented by ratios Ca:Mg:Fe=0.0:69.4:30.6 and the iron content in orthopyroxene is about 25 atomic%. These data together with results of preliminary petrographic observations indicate that Yamato-74646 is an $LL_{5,6}$ chondrite. The bulk chemical composition of this chondrite is given in Table 1.

Table 2. Basic magnetic properties of five achondrites (temperature=20°C).

Magnetic parameter	Yamato -74037	Yamato -74159	Yamato -74450	Yamato -75032	Yamato -7308(*l*)	Unit
Saturation magnetization (I_s)	0.32	0.061	0.22	0.042	0.53	emu/gm
Saturation remanence (I_R)	—	0.004	0.0044	0.0065	0.0027	emu/gm
Coercive force (H_c)	—	265	58	93	13	Oe
Remanence coercive force (H_{Rc})	—	420	72	320	—	Oe

Table 3. Magnetic parameters of chondrites.

Parameters of metallic component	Yamato-74362 (L)	Yamato-74646 (LL)
I_s	8.1	3.2 (emu/gm)
$I_s(\alpha)/I_s$	81	19 (%)
$I_s(\alpha+\gamma)/I_s$	19	7 (%)
$I_s(\gamma)/I_s$	0	74 (%)
Ni°/(Fe°+Ni°)	11.4	31.0 (wt. %)

The basic magnetic properties of the two chondrites have been examined in detail by NAGATA (1978). In a magnetic classification scheme for stony meteorite proposed by him, the saturation magnetization (I_s), ratios of magnetizations of α-, ($\alpha+\gamma$)- and γ-phases to the total saturation magnetization (*i.e.* $I_s(\alpha)/I_s$, $I_s(\alpha+\gamma)/I_s$ and $I_s(\gamma)/I_s$), and the Ni-content in metallic component derived from the magnetic analysis (Ni°/(Fe°+Ni°)) are taken as the key parameters. The observed values of these parameters of metallic component of the two chondrites are summarized in Table 3. In regard to I_s-values, allowable ranges for L- and LL-chondrites are $8<I_s<22$ emu/gm and $2<I_s<6$ emu/gm respectively. In regard to Ni°/(Fe°+Ni°) which can be derived from $I_s(\alpha)/I_s$, $I_s(\alpha+\gamma)/I_s$ and $I_s(\gamma)/I_s$, allowable ranges for L- and LL-chondrites are 10<Ni°/(Fe°+Ni°)<15 wt.% and 20%<Ni°/(Fe°+Ni°) respectively. It is certain therefore that Yamato-74362 is an L-chondrite and Yamato-74646 is an LL-chondrite.

3. Natural Remanent Magnetization of the Fusion Crust of Achondrites

3.1. Experimental procedures

A specimen of approximately a rectangular column in shape, having a fusion crust surface on one end, is prepared for each meteorite sample. The original dark colored skin of fusion crust ranges from 0.3 to 0.6 mm in thickness. NRM and weight of the prepared samples are first measured. By use of a fine-grain

sandpaper, the fusion crust surface is scraped off by 0.05–0.1 mm in a non-magnetic space, and then NRM and weight of the sample with a reduced thickness of fusion crust are remeasured. The same process is successively repeated until the fusion crust is completely removed and the undisturbed interior part also comes under examination. Then, the intensity and direction of NRM can be expressed as a function of weight of scraped-off surface part (Δm) or approximate thickness (d) of the scraped-off surface part of each meteorite specimen.

3.2. *Yamato-75032* (*diogenite*)

The initial weight of examined specimen of this achondrite is 1.128 gm. In Fig. 1, the intensity and direction of residual NRM per sample are illustrated as a function of Δm. It is clearly shown in the figure that the surface skin part of about 0.4 mm in thickness, which comprises mostly the fusion crust, has anomalously strong NRM compared with an almost uniform NRM of the interior, and the direction of anomalously strong NRM of the fusion crust is in approximate agreement with that of the interior NRM, the average intensity of which is 4.9×10^{-6} emu/gm.

An approximate curve of NRM intensity distribution of the fusion crust part, derived from a full line curve in Fig. 1, is shown in Fig. 2. The specific intensity

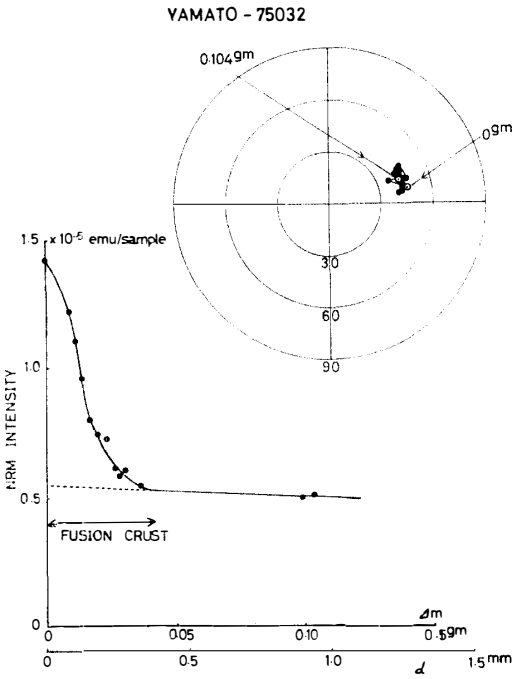

Fig. 1. Dependence of the intensity and direction of residual NRM upon the scraped off skin layer of Yamato-75032 achondrite.

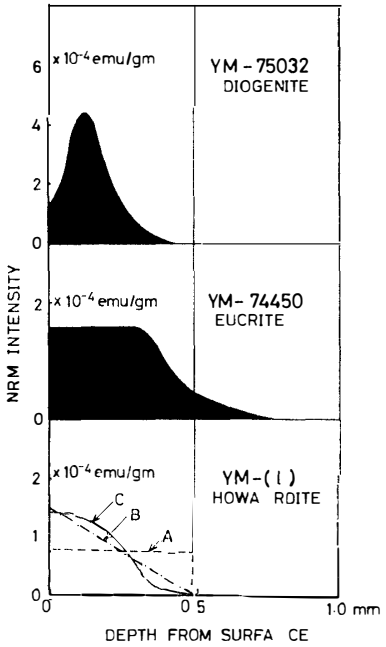

Fig. 2. Anomalous NRM distribution within the fusion crust of achondrites.
Top: Yamato-75032, middle: Yamato-74450 and bottom: Yamato-7308 (I).

of NRM sharply decreases from about d=0.13 mm to about d=0.45 mm. This result may suggest that the acquisition of thermoremanent magnetization (TRM) decreases inward from d=0.13 mm and is practically terminated at d=0.45 mm owing to a temperature distribution characteristic caused by the heat conduction. In the top surface part between d=0 and d=0.13 mm, however, the NRM intensity is considerably reduced from the maximum value at d=0.13 mm. There would be several possible mechanisms for the NRM reduction in the top surface part, but the most plausible mechanism would be an effect of ablation of metallic components in this part by overheating, as will be discussed later.

3.3. Yamato-74450 (eucrite)

The initial weight of an examined specimen is 1.184 gm. In Fig. 3, the intensity and direction of residual NRM per sample are illustrated as a function of Δm. In this case, the surface skin part of about 0.65 mm in thickness has anomalously strong NRM, but the direction of the surface skin NRM is different by about 45° from that of a uniform NRM of the interior part, which is 1.2×10^{-6} emu/gm in average intensity. Assuming then that the direction of surface skin NRM is constant but its intensity varies as a function of Δm, the intensity distribution of surface

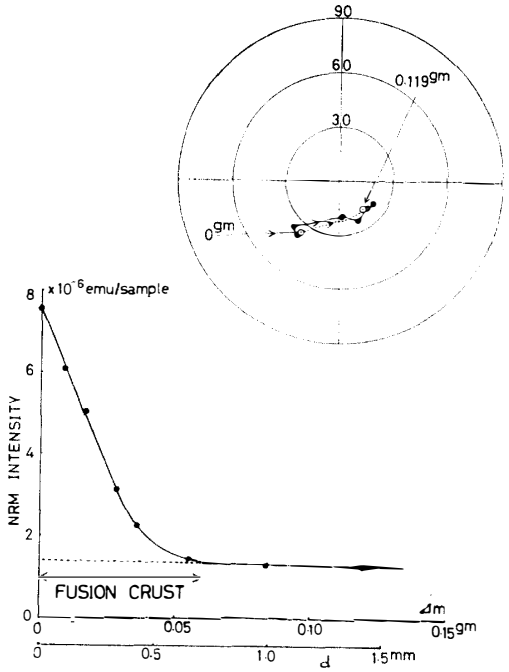

Fig. 3. Dependence of the intensity and direction of residual NRM upon the scraped off skin layer of Yamato-74450 achondrite.

skin NRM can be derived from the observed data shown in Fig. 3, the result being given in Fig. 2. Changes in NRM with Δm expected from the model is shown by a full line for the intensity and by a dotted line for the direction in Fig. 3.

The specific intensity of surface skin NRM is approximately constant from d=0 to about d=0.30 mm and it decreases with d from d=0.30 mm to d=0.80 mm. Actually, the average thickness of fusion crust of this sample is about 0.8 mm, being considerably thicker than that of Yamato-75032. The most plausible interpretation of the intensity distribution of fusion crust NRM of this sample might be that the top surface part of 0.3 mm in thickness was heated above Curie point, thus acquiring the total TRM, and the acquired partial TRM from d=0.30 mm to d=0.80 mm decreases with d owing to a temperature distribution characteristic caused by the heat conduction.

3.4. Yamato-7308(l) (howardite)

A preliminary analysis of the fusion crust NRM of this achondrite has already been reported (NAGATA and SUGIURA, 1977). In the present study, however, the surface skin NRM of this sample also has been re-examined in comparison with that of other achondrites. The initial weight of an examined sample is 2.060 gm. In Fig. 4, the intensity and direction of residual NRM per sample are shown as

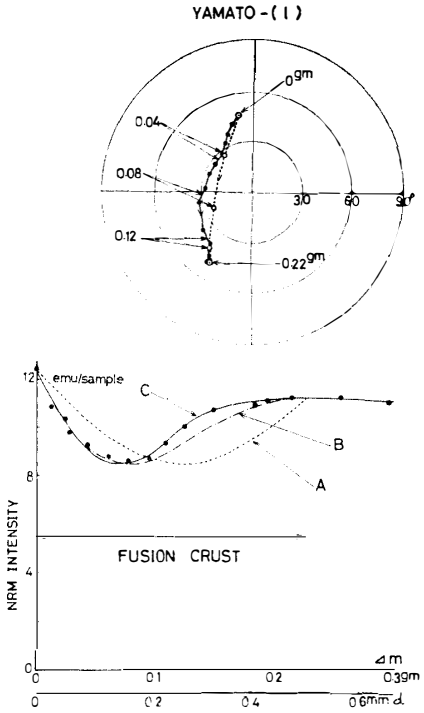

Fig. 4. Dependence of the intensity and direction of residual NRM upon the scraped off skin layer of Yamato-7308 (I) achondrite. Curves A, B and C in the NRM intensity versus the scraped off mass (Δm) or the scraped off thickness (d) correspond respectively to Models A, B and C in Fig. 2.

a function of Δm. In this case, the direction of residual NRM changes markedly with Δm from $\Delta m=0$ to about $\Delta m=0.22$ gm (*i.e.* $d=0.49$ mm), while the intensity of residual NRM also is gradually reduced from $d=0$ to $d=0.18$ mm and then is gradually recovered from $d=0.18$ mm to $d=0.50$ mm. These changes in the intensity and direction of residual NRM are attributable to an effect of removal of anomalous NRM of the fusion crust layer.

Although the path of changes in the NRM direction, shown in Fig. 4, is of a little zigzag form, the direction of additional fusion crust NRM may be assumed to be constant as an approximation of the first order. From the observed data of residual NRM for $d=0.50$–0.65 mm, the direction and specific intensity of the interior NRM can be determined, where the total thickness of anomalously magnetized fusion crust can be approximately estimated to be 0.50 mm.

In the case of Fig. 4, the approximate direction and intensity of the interior NRM (corresponding to $\Delta m=0.225$ gm or $d=0.50$ mm) are given by $\theta_0=50°$, $\varphi_0=60°$ and $I_0=11.30\times10^{-6}$ emu, while those of the additional fusion crust by

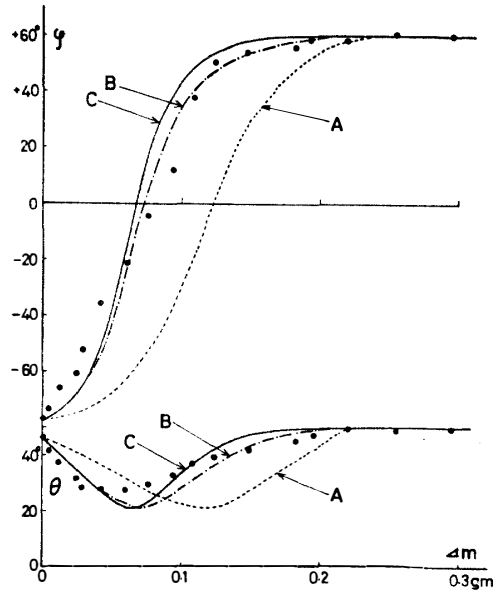

Fig. 5. Comparison of the direction of residual NRM of Models A, B and C with the observed value in θ and φ in spherical coordinates, after scraping off the skin layer by Δm in mass.

$\theta^*=85°$, $\varphi^*=-100°$, and $I^*=16.56\times10^{-6}$ emu, and those of the resultant total NRM corresponding to $d=0$ are given by $\theta=46°$, $\varphi=-79°$ and $I=12.36$ emu. Then, the specific intensity of the uniform interior NRM is 6.3×10^{-6} emu/gm, and the direction of fusion crust NRM makes an angle of 131° with the direction of interior NRM.

As for the distribution of the fusion crust NRM intensity, three models are assumed in the present study. They are (A) a uniform distribution from $\Delta m=0$ to $\Delta m=0.225$ gm, where the average NRM intensity is 7.34×10^{-5} emu/gm, (B) a linear decrease of NRM intensity with Δm from 1.47×10^{-4} emu/gm at $\Delta m=0$ to 0 at $\Delta m=0.225$ gm, and (C) a decreasing curve of NRM intensity with Δm as shown at the bottom of Fig. 2, which is the most fittable to observed data of the residual NRM intensity as shown in Fig. 4, where the NRM intensity at $\Delta m=0$ is given by 1.41×10^{-4} emu/gm.

The observed data of intensity and direction of the residual NRM are plotted respectively as functions of Δm in Fig. 4 and by θ and φ in Fig. 5, while those of Models A, B and C also are shown in Figs. 4 and 5. As illustrated in Fig. 4, the observed change of NRM intensity with Δm is well represented by Model C, whereas the observed change of NRM direction with Δm is approximately represented by both Models B and C almost equally, as shown in Fig. 5. A systematic discrepancy between the observed data and the theoretical curves for Models C and B in Fig. 5

may be mostly due to the simple assumption that the direction of additional fusion crust NRM is constant. At the top of Fig. 4, changes of residual NRM direction with Δm for Model C are illustrated by a dotted curve in comparison with the observed data.

It is certain in these analyses that the direction of fusion crust NRM is not exactly constant, but it can be considered approximately constant. Then, Model C can reasonably well represent the intensity distribution of fusion crust NRM of this sample. Namely, the top surface part of about 0.15 mm in thickness was heated above Curie point, acquiring the total TRM, and TRM from d=0.15 mm to d= 0.50 mm decreases with d owing to a temperature distribution characterized by the heat conduction from the surface.

3.5. Yamato-74037 (diogenite)

The initial weight of an examined specimen of this diogenite was 1.145 gm. The intensity and direction of residual NRM as a function of Δm is illustrated in Fig. 6. It may be concluded in this figure that the direction of fusion crust NRM is in approximate agreement with that of a uniform interior NRM within a limit of possible errors. Assuming that the direction of fusion crust NRM is coincident with that of interior NRM, the specific intensity of fusion crust NRM dependent on Δm and consequently on d has been derived as shown in the top diagram of

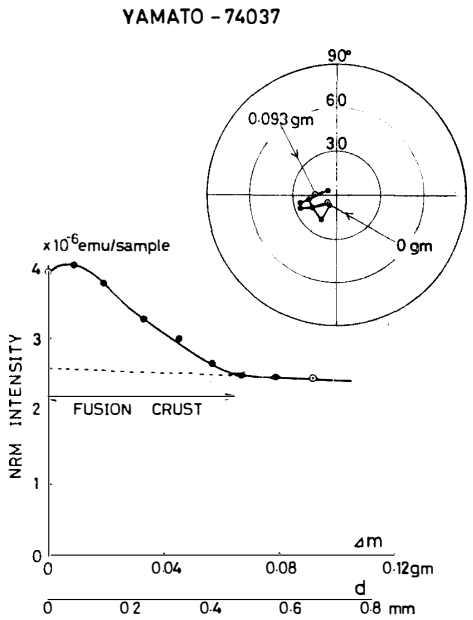

Fig. 6. Dependence of the intensity and direction of residual NRM upon the scraped off skin layer of Yamato-74037 achondrite.

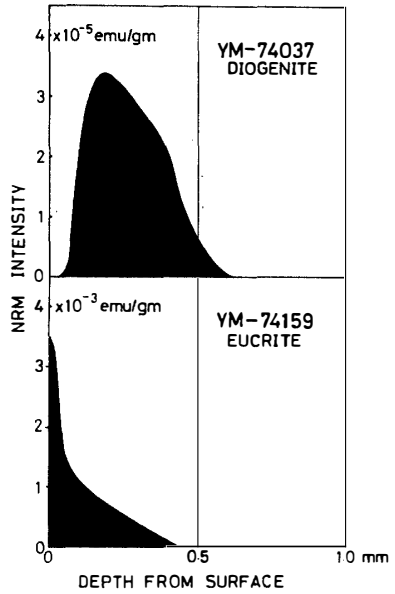

Fig. 7. Anomalous NRM distribution within the fusion crust of achondrites.

Fig. 7. The top surface layer from $d=0$ to $d=0.08$ mm has practically no NRM, while the maximum NRM intensity of 3.4×10^{-5} emu/gm takes place at $d=0.2$ mm, the NRM intensity decreasing inward from $d=0.2$ mm to $d=0.6$ mm. The observed lack of NRM within the top surface layer may be due to an effect of ablation of metallic components in this layer as in the case of Yamato-75032. Since the average specific intensity of uniform interior NRM is 2.3×10^{-6} emu/gm, the fusion crust NRM of this achondrite also is much stronger than its interior NRM.

3.6. Yamato-74159 (eucrite)

The initial weight of an examined sample of this eucrite was 2.246 gm. The intensity and direction of residual NRM as a function of Δm is illustrated in Fig. 8. As shown in the figure, the initial direction of NRM of this sample with a fusion crust (for $\Delta m=0$) is different by 45° in angle from that of the interior NRM corresponding to $\Delta m=0.222$ gm. If we assume that the direction of fusion crust NRM is constant, then an angle between the fusion crust NRM and the interior NRM is estimated to be 54°, (Model 1). The specific intensity of fusion crust NRM dependent on Δm, which is the most fittable to observed data in Model 1, is given by a curve of J_n (Model 2 and 1) shown in Fig. 9, where changes in the direction of residual NRM as a function of Δm calculated for Model 1, θ and φ, also are illustrated. Agreements of J_n and φ curves of Model 1 with observed data

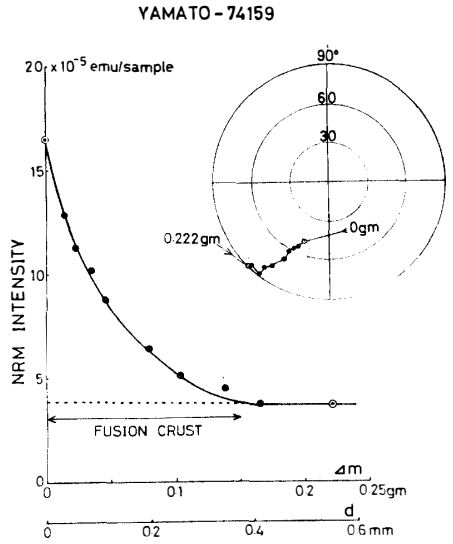

Fig. 8. Dependence of the direction and intensity of residual NRM upon the scraped off skin layer of Yamato-74159 achondrite.

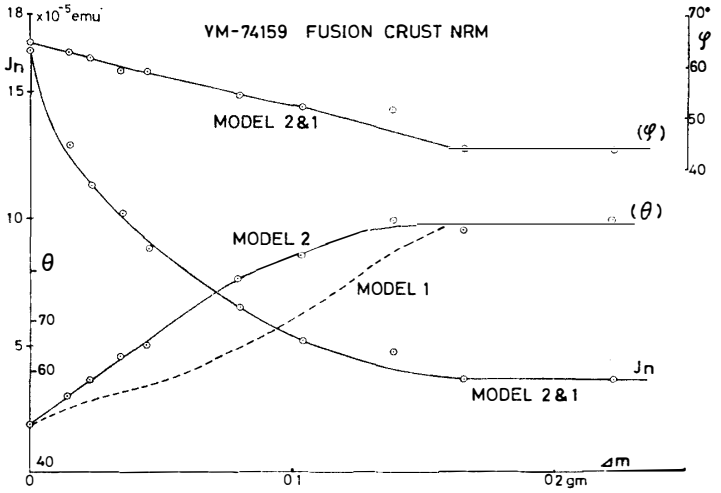

Fig. 9. Comparison of the direction of residual NRM of Models 1 and 2 with the observed value, in θ and φ in spherical coordinates, after scraping off the skin layer by Δm in mass.
Model 1: Direction of the fusion crust NRM assumed constant.
Model 2: Direction of the fusion crust NRM assumed changed as illustrated in Fig. 10.

may be considered reasonably satisfactory, but θ curve of Model 1 is considerably deviated from observed θ-values.

This result may suggest that the direction of fusion crust NRM considerably changes for various values of depth, d. In Model 2, therefore, it is assumed that

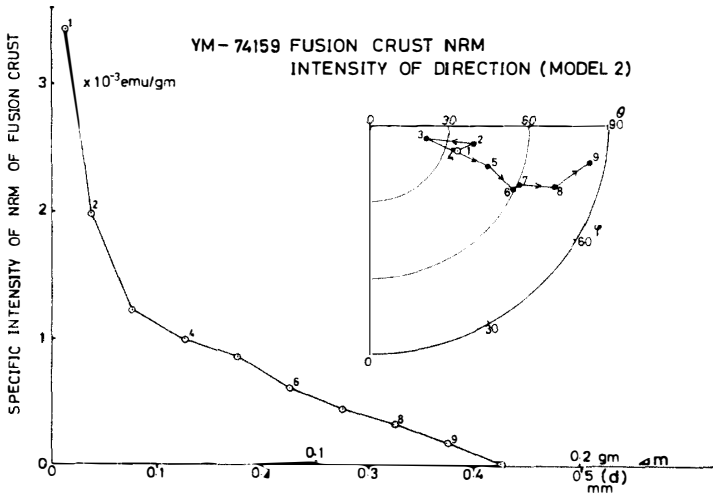

Fig. 10. Distribution of direction and intensity of anomalous NRM within the fusion crust of Yamato-74159.

both the intensity and direction of fusion crust NRM change with Δm so that resultant values of J_n, θ and φ change with Δm (or with d) as represented by respective full line curves given in Fig. 9. The specific intensity and direction of fusion crust NRM thus estimated for Model 2 are given as a function of d in Fig. 10. In this case, the distribution of specific intensity of fusion crust NRM with d is practically the same as that for Model 1, but its direction changes with d from the surface to the bottom of anomalously magnetized skin layer (*i.e.* d= 0.43 mm) by about 60° in angle. It may have to be emphasized, however, that the estimated rotation angle of fusion crust NRM from the top to the bottom of anomalously magnetized skin layer is not more than 60°. The specific intensity of fusion crust NRM, shown in Figs. 7 and 10, decreases sharply with d from d=0 to about d=0.08 mm and then gradually to d=0.43 mm.

4. Natural Remanent Magnetization of the Fusion Crust of Ordinary Chondrites

The intensity and direction of NRM of Yamato-74362 (L_5 chondrite) and Yamato-74646 ($LL_{5,6}$ chondrite) are illustrated as a function of Δm in Figs. 11 and 12 respectively, where the initial sample weights of Yamato-74362 and -74646 are 12.70 gm and 1.819 gm respectively. Although it seems that NRM of the surface skin part is somewhat anomalous compared with the interior NRM in both cases, the additional fusion crust NRM is not so conspicuous as in the cases of the five achondrites.

As shown in Fig. 11, the direction of residual NRM (after a scraping of the surface skin down to d) of Yamato-74362 is approximately constant from d=0

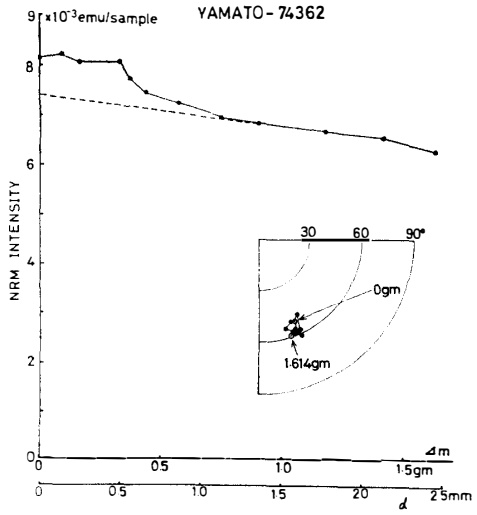

Fig. 11. Dependence of the intensity and direction of residual NRM upon the scraped off skin layer of Yamato-74362 chondrite.

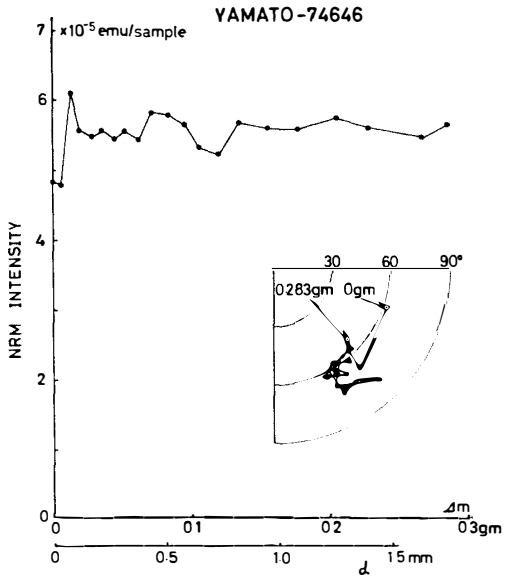

Fig. 12. Dependence of the intensity and direction of residual NRM upon the scraped off skin layer of Yamato-74646 chondrite.

to d=0.5 mm, so that the direction of a possible fusion crust NRM should be in approximate agreement with that of the interior NRM. Roughly speaking, the intensity of residual NRM is nearly constant from d=0 to d=0.5 mm. This result may suggest that the fusion crust of this outermost skin of about 0.5 mm in thickness has a very weak NRM, probably because the metallic component in this part has

Table 4. Surface-skin NRM of Yamato-74646 chondrite.

Δm (gm)	I_n (emu/sample)	θ (degree)	φ	I_{FC} (emu/gm)	Θ (degree)	Φ
0	440.8×10^{-7}	61.3	30.7			
				4.24×10^{-3}	102	−70
0.0050	438.1×10^{-7}	67.6	00.5			
				2.83×10^{-3}	32	07
0.0120	610.2×10^{-7}	56.8	01.8			
				0.84×10^{-3}	119	−143
0.0193	557.9×10^{-7}	56.9	1–102.0			

been subjected to a strong ablation effect caused by overheating.

A considerable decrease of residual NRM with d from d=0.5 mm to d=1.2 mm suggests that a rate of TRM acquisition exponentially decreases from about 8.5×10^{-3} emu/gm at d=0.5 mm to about 0.6×10^{-3} emu/gm at d=1.2 mm. For comparison, the average intensity of interior NRM of this chondrite is 5.8×10^{-4} emu/gm. It may thus be considered that the surface skin of this chondrite is composed of a very weakly magnetized outermost surface layer of 0.5 mm in thickness and an inner layer of about 0.7 mm in thickness which is anomalously magnetized as mentioned above.

As shown in Fig. 12, the surface skin NRM of Yamato-74646 changes considerably in its intensity and direction in a thin layer from d=0 to d=0.19 mm. A plausible interpretation of the observed change of the surface skin NRM would be an effect of a rotation of the meteorite during the process of TRM acquisition. Results of a vector-differentiation analysis of the first 4 measurements of the residual NRM of this sample is given in Table 4, where I_n, θ and φ are the residual NRM intensity and its direction respectively for the corresponding values of Δm, while I_{FC}, Θ and Φ represent respectively the average specific intensity of NRM and its average direction for surface skin layers between the successive Δm values. It may be seen in Table 4 that the specific intensity of NRM decreases with the depth from the surface, whereas the NRM direction indicates a tendency of a rotation of the sample.

Since the size of individual metallic grains holding NRM in ordinary chondrites often range from 0.1 mm to 0.5 mm, which are comparable with the fusion crust thickness, the present analysis method of the fusion crust NRM based on an assumption that the magnetic property distribution is practically uniform within a meteorite piece may not be sufficiently applied for the ordinary chondrites. This is the main reason why only qualitative discussions are made on the fusion crust NRM of ordinary chondrites in the present study.

5. General Characteristics of Fusion Crust NRM of Achondrites

As summarized in Table 5, the thickness of anomalously magnetized skin layer

Table 5. Summary of fusion crust NRM of achondrites.

Parameter \ Sample	Yamato -74037 (Diogenite)	Yamato -74159 (Eucrite)	Yamato -74450 (Eucrite)	Yamato -75032 (Diogenite)	Yamato -7308(*l*) (Howardite)	Unit
I°_{FC}	3.4×10^{-5}	3.3×10^{-3}	1.6×10^{-4}	4.5×10^{-4}	1.4×10^{-4}	emu/gm
I°_n	2.3×10^{-6}	1.8×10^{-5}	1.25×10^{-6}	5.3×10^{-6}	6.3×10^{-6}	emu/gm
d_0	0.6	0.4	0.8	0.4	0.5	mm
I_s	0.318	0.061	0.215	0.042	0.53	emu/gm
H_c	—	265	58	93	13	Oe
I_{FC}/I°_n	15	183	128	85	22	

I°_{FC}: Maximum specific intensity of fusion crust NRM.
I°_n : Specific intensity of uniform interior NRM.
d_0 : Thickness of anomalously magnetized skin layer.
I_s : Saturation magnetization of uniform interior.
H_c : Coercive force of uniform interior.

of achondrites ranges from 0.4 mm to 0.8 mm, which are in approximate agreement with the thickness of dark colored fusion crust layer of each achondrite. The direction of fusion crust NRM is approximately constant or changes not more than 60° in angle within the anomalously magnetized skin layer, and the intensity of fusion crust NRM exponentially decreases inward within a range of 0.3–0.4 mm from the bottom of anomalously magnetized layer in all five examined achondrites. However, the distribution behavior of fusion crust NRM intensity (I_{FC}) from the surface to 0.2–0.4 mm in depth is considerably different in different samples of achondrite. For two achondrites (Yamato-74450 and Yamato-7308(l)), I_{FC} is approximately constant within the top surface layer, whereas I_{FC} increases with d for two other achondrites (Yamato-75032 and Yamato-74037) and it sharply decreases with d for an achondrite (Yamato-74159) within the surface layer.

These characteristics of fusion crust NRM of achondrites may be closely related to the acquisition mechanism of the remanent magnetization. It would be almost certain that the fusion crust NRM was acquired by the surface skin layer as TRM or pTRM in the course of cooling from a certain high temperature in the presence of geomagnetic field on entry of the achondrites into the earth's atmosphere, because the particular NRM is geometrically confined only to the fusion crust layer. However, an exact mechanism for the acquisition of TRM or pTRM does not seem to be simple, because the conversion processes of kinetic and potential energies of meteorites incoming from the outer space into the earth's atmosphere are associated with various complicated phenomena such as melting and ablation of the outer layer of meteorites, forming a shock-front surface in the atmosphere, heating and ionization of the neighboring atmosphere, and heat conduction and radiation from the outer layer of meteorites and the neighboring atmospheric gas. For example,

a simple hypothesis that the interior of a solid achondrite was heated up by the heat conduction from its fixed surface of θ_0 in temperature during t in time and then cooled down in the presence of a magnetic field does not well stand for the observed characteristics of fusion crust NRM. Assuming one dimensional heat conduction of a semi-infinite body of K^2 in the thermal diffusivity under an initial condition that temperature $\theta=0°C$ for $t<0$ and a boundary condition that $(\theta)_{d=0}=\theta_0$ for $t\geq 0$, temperature θ at depth d at time $t=t$ is given by

$$\frac{\theta}{\theta_0}=\mathrm{Erfc}\left(\frac{d}{2K\sqrt{t}}\right). \qquad (1)$$

The thermal diffusivity defined as

$$K^2\equiv k/C\rho \qquad (2)$$

where k=thermal conductivity, C=heat capacity and ρ=density, can be evaluated for stony meteorites on the basis of observed data such as $k=(3.6\text{–}5.5)\times 10^{-3}$ cal·s^{-1}, cm^{-1}, deg^{-1} (ALEXEYEVA, 1960) and $C=(0.166\text{–}0.182)$ cal·gm^{-1},deg^{-1}, (ALEXEYEVA, 1958) and measured value of $\rho=3.3$ gm·cm^{-3}. Taking the average values of k, C, and ρ, K^2 of stony meteorites is about 8.1×10^{-3} cm^2·s^{-1}. As for θ_0, the melting temperatture of stony meteorites, *i.e.* 1320–1410°C, could be adopted, because the surface of a fusion crust is a product of remelting of a stony meteorite.

As example of estimation of θ with the aid of eq. (1) for a stony meteorite having the material constants mentioned above is illustrated in Fig. 13 for the case of $t=1$ s. Even in the case of $t=1$ s, $\theta=903°C$ at $d=1$ mm, $\theta=562°C$ at $d=2$ mm and $\theta=24°C$ at $d=3$ mm. For $t=10$ s, $\theta=1045°C$ at $d=1$ mm, $\theta=805°C$ at $d=2$ mm, $\theta=417°C$ at $d=4$ mm and $\theta=202°C$ at $d=6$ mm. As a falling meteorite surface is heated up to its melting temperature during at least several seconds, the

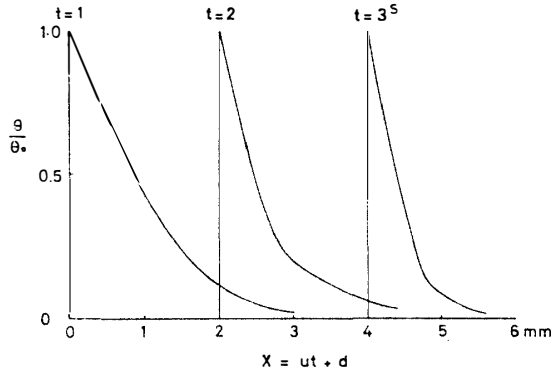

Fig. 13. Temperature distribution from a moving surface of temperature θ_0 for a one-dimensional chondrite model.

surface-skin layer several mm thick at least must have been heated to a temperature sufficient to acquire TRM. For example, the partial TRM acquisition curve for Yamato-7307 (NAGATA *et al.*, 1976) has indicated that its TRM is mostly acquired during cooling from 800°C to 400°C. Then, the surface-layer of this achondrite from the surface to d=4 mm may have acquired a significant amount of TRM, provided that t assumes 10 s. The observed thickness of the anomalously magnetized surface-skin layer of achondrites is smaller than 1 mm.

It has been established, on the other hand, that the surface of a falling meteorite is subjected to the ablation caused by a vaporization of the molten surface for a period from 4 s to over 1 min. Results of several theoretical studies on this problem have indicated that the meteorite surface layer is lost by the ablation with a rate of 1–4 mm per second of the flight (*e.g.* BUCHWALD, 1975). If the ablation rate is sufficiently large in comparison with the inward heat conduction rate, then the thickness of a remaining surface-skin layer, which is heated up sufficiently to acquire TRM, may have to be much reduced.

A theoretical treatment of this problem is much complicated, because the heat source boundary is moving, and temperature at the heat source boundary is changing. In order to semi-quantitatively estimate the effect of ablation, a simple one dimensional model of a constant surface temperature and a constant speed of the inward moving of the surface boundary will be discussed.

It will take a certain time after the entry into the atmosphere to heat up the surface to begin the ablation, and the heat conduction into the interior will take place during the time. In the present treatment, this condition is simply represented by a heat conduction from a fixed surface of a constant temperature (θ_0) during t^* in time, which can be evaluated by eq. (1). Then, the ablation will start at $t=t^*$, resulting in an inward movement of the surface plane of θ_0 in temperature with constant speed (u.) This second process will be theoretically followed by a numerical integration of the one dimensional heat conduction equation, namely,

$$\frac{\delta\theta}{\delta t}=K^2\frac{\delta^2\theta}{\delta x^2} \qquad \text{with} \qquad [\theta]_{x=ut}=\theta_0,\ (x\geqq ut). \tag{3}$$

Fig. 13 illustrates an example of the temperature distribution within a solid stony meteorite thus evaluated for t^*=1 s and u=2 mm/s. Since the convergence characteristics of the numerical integration of the heat conduction equation is not sufficiently good in the present computation, a quantitative discussion of the present result may not be allowed. It is seen qualitatively in Fig. 13, however, that the temperature gradient in the surface skin layer becomes considerably larger with an inward proceeding of the surface of a constant temperature (θ_0) with u in speed.

After a certain time from the start of the surface ablation, therefore, the thickness of surface-skin layer, which is heated up to a temperature sufficient to

acquire TRM, may become smaller than 1 mm. In the case of Fig. 13, for example, θ/θ_0 becomes 0.1 at d=2.1 mm at t=1 s, but θ/θ_0 becomes 0.1 at d=0.95 mm at t=3 s. In the case of u=2 mm/s, the distribution of θ/θ_0 with d for t=3 s is practically close to the asymptotic distribution. When t^* is larger than 1 s, it takes a longer time to reach the asymptotic distribution of θ/θ_0. If u is larger than 2 mm/s, on the other hand, the temperature gradient becomes sharper than that illustrated in Fig. 13 for the same value of t^*. The observed fact that the surface skin layer, which is anomalously magnetized, is considerably smaller than 1 mm may therefore suggest that the ablation rate of the surface of those examined achondrites was equal to or larger than 2 mm/s.

The ablation of the falling meteorite surface is associated with the emission of vaporized surface materials. If the content of metallic component in the surface skin layer remains the same as that in the interior, the acquired TRM intensity will be constant in the top surface layer where the maximum temperature is above Curie point, and will decrease with depth in accordance with a decrease of the maximum temperature from Curie point. This would be the case of Yamato-74450 and Yamato-7308(*l*).

If the metallic component in the remaining thin layer close to the surface is much reduced in comparison with the silicate components during the vaporization process, the top surface parts of a fusion crust have much smaller TRM compared with the inner parts of the fusion crust. This would be the case of Yamato-75032 and Yamato-74037. If, on the contrary, the vaporization of the surface is stopped when the metallic component is concentrated near the surface, then the TRM acquisition of the top surface parts will be larger than that of the inner parts. This would be a probable interpretation of the NRM distribution in the fusion crust of Yamato-74159.

Since the surface parts of a falling meteorite are molten and partly vaporized, dependent on the surface positions, the distribution characteristics of NRM in the surface skin layer may not be simply interpreted.

References

ALEXEYEVA, K. N. (1958): Physical properties of stony meteorite and their interpretation in the light of hypothesis regarding the origin of meteorites (in Russian). Meteoritika, **16**, 67–77.

ALEXEYEVA, K. N. (1960): New data on the physical properties of stony meteorites (in Russian). Meteoritika, **18**, 68–76.

BUCHWALD, V. F. (1975): Handbook of Iron Meteorites, Vol. 1: Iron Meteorites in General. Barkeley, Univ. California Press, 243 p.

BUTLER, R. F. (1972): Natural remanent magnetization and thermomagnetic properties of the Allende meteorite. Earth Planet. Sci. Lett., **17**, 120–128.

NAGATA, T. (1979): Magnetic classification of Antarctic stony meteorites (III). Mem. Natl Inst.

Polar Res., Spec. Issue, **12**, 223–237.
NAGATA, T. and SUGIURA, N. (1977): Paleomagnetic field intensity derived from meteorite magnetization. Phys. Earth Planet. Inter., **13**, 373–393.
TAKEDA, H., MIYAMOTO, M., YANAI, K. and HARAMURA, H. (1978): A preliminary mineralogical examination of the Yamato-74 achondrites. Mem. Natl Inst. Polar Res., Spec. Issue, **8**, 170–184.
WEAVING, B. (1962): The magnetic properties of the Brewster meteorite. Geophys. J., **7**, 203–211.
YAGI, K., LOVERING, J. F., SHIMA, M. and OKADA, A. (1978): Mineralogical and petrographical studies of the Yamato meteorites, Yamato-7301(j), -7305(k), -7308(l) and -7303(m) from Antarctica. Mem. Natl Inst. Polar Res., Spec. Issue, **8**, 121–141.
YANAI, K., MIYAMOTO, M. and TAKEDA, H. (1978): A classification for the Yamato chondrites based on the chemical compositions of their olivines and pyroxenes. Mem. Natl Inst. Polar Res., Spec. Issue, **8**, 110–120.

(*Received April 24, 1979*)